

On-Scalp Optically Pumped Magnetometers versus Cryogenic Magnetoencephalography for Diagnostic Evaluation of Epilepsy in School-aged Children

Odile Feys, MD • Pierre Corvilain, PhD • Alec Aebly, MD, PhD • Claudine Sculier, MD • Florence Christiaens, MD • Niall Holmes, PhD • Matthew Brookes, PhD • Serge Goldman, MD, PhD • Vincent Wens, PhD • Xavier De Tiège, MD, PhD

From the Departments of Neurology (O.F.), Pediatric Neurology (C.S., F.C.), Nuclear Medicine (S.G.), and Translational Neuroimaging (V.W., X.D.T.), CUB Hôpital Erasme, Université Libre de Bruxelles, Brussels, Belgium; Laboratory of Translational Neuroimaging and Neuroanatomy (Laboratoire de Neuroimagerie et Neuroanatomie translationnelles) (LN²T), ULB Neuroscience Institute, Université Libre de Bruxelles, 808 Lennik St, Brussels, Belgium (O.F., P.C., S.G., V.W., X.D.T.); Department of Pediatric Neurology, Hôpital Universitaire des Enfants Reine Fabiola, Université Libre de Bruxelles, Brussels, Belgium (A.A.); and Sir Peter Mansfield Imaging Centre, School of Physics and Astronomy, University of Nottingham, Nottingham, United Kingdom (N.H., M.B.). Received September 30, 2021; revision requested December 21; final revision received February 23, 2022; accepted March 2. **Address correspondence to** O.F. (email: odile.feys@ulb.be).

Supported by the Fonds Erasme (Research Conventions “Les Voies du Savoir” and “Projet de recherche clinique à des techniques médicales émergentes 2020”) and the Fonds de la Recherche Scientifique (FRS-FNRS) (Equipment credit: U.N013.21F). O.F. supported by a research grant from the Fonds pour la Formation à la Recherche dans l’Industrie et l’Agriculture (FRIA, FRS-FNRS, Brussels, Belgium). P.C. supported by a research grant from the Fonds Erasme (Research Convention “Alzheimer,” Brussels, Belgium). M.B. received a grant from Engineering and Physical Sciences Research Council, UK Quantum Technology Hub in Sensing and Timing.

Conflicts of interest are listed at the end of this article.

See also the editorial by Widjaja in this issue.

Radiology 2022; 000:1–6 • <https://doi.org/10.1148/radiol.212453> • Content code: **PD** • © RSNA, 2022

Background: Magnetoencephalography (MEG) is an established method used to detect and localize focal interictal epileptiform discharges (IEDs). Current MEG systems house hundreds of cryogenic sensors in a rigid, one-size-fits-all helmet, which results in several limitations, particularly in children.

Purpose: To determine if on-scalp MEG based on optically pumped magnetometers (OPMs) alleviates the main limitations of cryogenic MEG.

Materials and Methods: In this prospective single-center study conducted in a tertiary university teaching hospital, participants underwent cryogenic (102 magnetometers, 204 planar gradiometers) and on-scalp (32 OPMs) MEG. The two modalities for the detection and localization of IEDs were compared. The *t* test was used to compare IED amplitude and signal-to-noise ratio (SNR). Distributed source modeling was performed on OPM-based and cryogenic MEG data.

Results: Five children (median age, 9.4 years [range, 5–11 years]; four girls) with self-limited idiopathic (*n* = 3) or refractory (*n* = 2) focal epilepsy were included. IEDs were identified in all five children with comparable sensor topographies for both MEG devices. IED amplitudes were 2.3 (7.2 of 3.1) to 4.6 (3.2 of 0.7) times higher (*P* < .001) with on-scalp MEG, and the SNR was 27% (16.7 of 13.2) to 60% (12.8 of 8.0) higher (*P* value range: .001–.009) with on-scalp MEG in all but one participant (*P* = .93), whose head movements created pronounced motion artifacts. The neural source of averaged IEDs was located at approximately 5 mm (*n* = 3) or higher (8.3 mm, *n* = 1; 15.6 mm, *n* = 1) between on-scalp and cryogenic MEG.

Conclusion: Despite the limited number of sensors and scalp coverage, on-scalp magnetoencephalography (MEG) based on optically pumped magnetometers helped detect interictal epileptiform discharges in school-aged children with epilepsy with a higher amplitude, higher signal-to-noise ratio, and similar localization value compared with conventional cryogenic MEG.

Online supplemental material is available for this article.

© RSNA, 2022

Drug-resistant epilepsy occurs in one-third of patients with epilepsy (1). The main treatment to alleviate seizures in those patients is epilepsy surgery, provided that the presumed location of the epileptogenic zone (PLEZ) is focal, well localized, and does not involve functionally eloquent cortices (1). Magnetoencephalography (MEG) provides nonredundant information for the noninvasive localization of the PLEZ in patients with refractory focal epilepsy (RFE) (2,3).

Cryogenic MEG systems house hundreds of superconducting quantum interference devices (SQUIDs) in a rigid, one-size-fits-all helmet (4). SQUIDs have several major limitations (4). Due to cryogenic cooling, a thermally insulated

gap is required between the scalp and SQUIDs, meaning that the brain-to-sensor distance is approximately 2–5 cm in adults who fit the system well and larger in patients with small heads, such as children. Small head size increases the brain-to-sensor signal attenuation as magnetic fields decrease with the square of the distance. Pediatric SQUID-based MEG (hereafter, SQUID-MEG) systems do not fully alleviate those limitations as they restrict the use of MEG to specific age ranges (eg, infants or school-aged children) (5).

Optically pumped magnetometers (OPMs) are cryogenic-free magnetic field sensors. OPMs can be placed directly on the scalp to record neuromagnetic signals with an

Abbreviations

EEG = electroencephalography, IED = interictal epileptiform discharge, MEG = magnetoencephalography, OPM = optically pumped magnetometer, PLEZ = presumed location of the epileptogenic zone, RFE = refractory focal epilepsy, SNR = signal-to-noise ratio, SQUID = superconducting quantum interference device

Summary

On-scalp optically pumped magnetometer-based magnetoencephalography provided a higher amplitude and signal-to-noise ratio than cryogenic magnetoencephalography, with similar localization value, for interictal epileptic discharges in school-aged children with focal epilepsy.

Key Results

- In this prospective study, on-scalp optically pumped magnetometer (OPM)-based magnetoencephalography (MEG), hereafter OPM-MEG, helped detect interictal epileptic discharges (IEDs) in five school-aged children with idiopathic or refractory focal epilepsy.
- OPM-MEG provided higher IED amplitude (2.3–4.6 times higher, $P < .001$) and signal-to-noise ratio (27%–60% higher, P value range: .001–.009) than conventional cryogenic MEG, with similar localization value.

adequate level of noise, even during motion (4). Consequently, OPM arrays can adapt to any head shape or size and record human brain activity in natural conditions (4). On-scalp OPM-based MEG (hereafter, OPM-MEG) should substantially improve the signal-to-noise ratio (SNR) and spatial resolution of MEG, especially in children (4).

OPM-MEG recording (15 OPMs with a bespoke three-dimensional-printed scanner cast that housed the OPMs) has been described in one adult patient with RFE (6). OPM-MEG was able to help detect and localize the source of interictal epileptic discharges (IEDs). To our knowledge, a direct comparison with SQUID-MEG has not been established in the literature.

We aimed to evaluate whether OPM-MEG can alleviate SQUID-MEG limitations by comparing IED recordings collected using 32 OPMs fixed on flexible electroencephalography (EEG)-like caps with recordings collected with SQUID-MEG in five children with focal epilepsy.

Materials and Methods

Participants and Study Design

Our prospective study was approved by the ethics committee of the CUB Hôpital Erasme (reference numbers P2019/426, B406201941248), and written informed consent was obtained from the child and their legal representative(s) prior to inclusion in the study.

From April 12 to June 25, 2021, we prospectively included children with focal epilepsy in a convenience sampling framework with the following inclusion criteria: (a) clinical follow-up in a tertiary university teaching hospital (CUB Hôpital Erasme and Hôpital Universitaire des Enfants Reine Fabiola), (b) frequent unifocal IEDs demonstrated on a previous clinical EEG, (c) ability to remain relatively still for at least 15 minutes of MEG recordings, and (d) written informed consent from the child and their legal representative(s) prior to inclusion in the study.

Imaging Procedures

OPM-MEG (Fig 1) was performed using 32 zero-field magnetometers (Gen-2.0, QuSpin; single-axis mode, gain 2.7 V per nanotesla [nT]) whose signals were fed to a digital acquisition unit (National Instruments; sampling rate of 1200 Hz, no band-pass filter). Three-dimensional-printed plastic sensor mounts (64 per EEG cap; Fig 1B) were sewn on conventional flexible EEG caps (EasyCap) (7,8), which were adapted to each child's head circumference according to the 10–10 EEG electrode system, to secure the OPMs closely to the scalp. This design was easy and quick (1–2 minutes) to place on the child's head and bypassed the need for any material between the scalp and cap that might be a source of discomfort (7). The mounts covered approximately 40% of the inferior part of the OPMs and had vertical openings (Fig 1C) to allow dissipation of OPM-related heat. Each mount was also equipped with one hollow at each corner of the base (Fig 1D) to allow digitization of the OPM position on the child's scalp using an electromagnetic tracker (Fastrak, Polhemus). Three small marks were also drawn on the child's forehead and EEG cap (one right, one middle, and one left) using a skin pencil to check that the cap did not move relative to the child's head during acquisition. Due to the limited number of OPMs, all sensors were placed on and around the PLEZ as determined with a previous scalp EEG; therefore, the whole head was not covered. Recordings took place inside a compact magnetically shielded room optimized for OPM recordings (OPM-compact MuRoom, Magnetic Shielded Limited; background magnetic field <15 nT after degaussing, length \times width \times height: 1.5 \times 1.5 \times 2 m, weight: 2000 kg) (Fig 1A). Children sat comfortably at the center of the magnetically shielded room and watched a movie with no constraints on head position or movement. No further field compensation (4) was applied. Sensor locations were obtained outside the magnetically shielded room after the recording and removal of OPMs by digitizing the four base points of each mount housing an OPM and at least 300 points (face and scalp) relative to anatomic fiducials. Removal of the OPMs was performed to avoid any movement of the EEG cap and OPM holders. The acceptance of OPM-MEG by the children and the operators was qualitatively assessed after the recordings.

SQUID-MEG (Fig 1E) was performed under similar conditions using a 306-channel, whole-scalp neuromagnetometer (Triux, MEGIN; 204 planar gradiometers, 102 magnetometers; sampling rate, 1000 Hz; band-pass filter, 0.1–300 Hz) placed in a lightweight magnetically shielded room (Maxshield, MEGIN; background magnetic field >200 nT, length \times width \times height: 4.25 \times 3 \times 2.5 m, weight: 5800 kg) (9). The child's head position was continuously tracked using four head position indicator coils. These coils, and 300 face and scalp points, were digitized relative to anatomic fiducials using the same electromagnetic tracker. In all participants, SQUID-MEG was performed just after the digitization of the OPM mounts.

Each participant underwent three-dimensional T1-weighted MRI of the brain (spatial resolution: 1 \times 1 \times 1 mm), either during their clinical assessment (1.5-T Intera system, Philips; $n = 3$, 3–11 months before MEG) or just after MEG (3-T Signa PET/MRI system, GE Healthcare; $n = 2$).

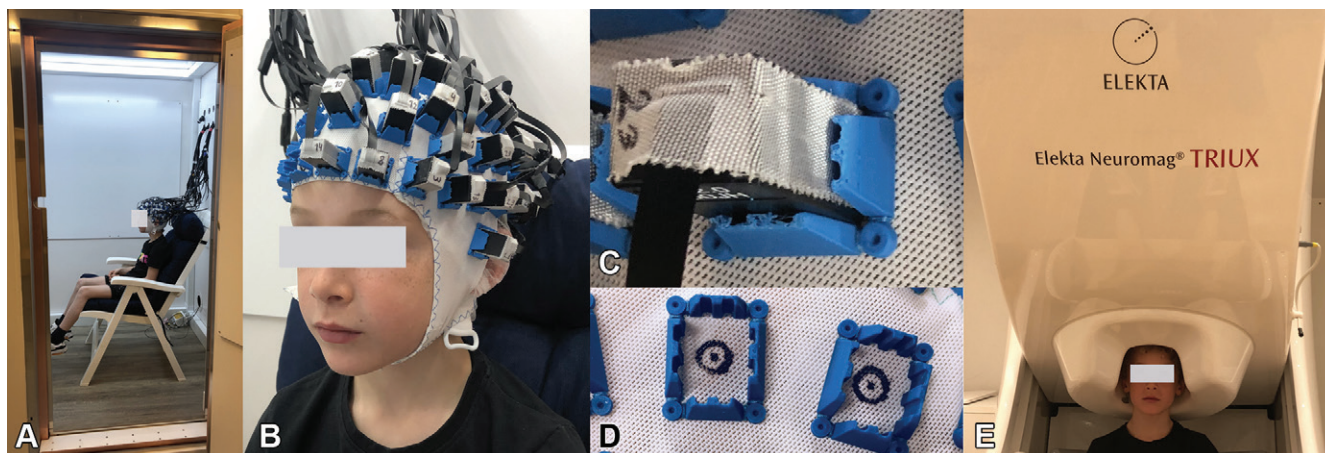


Figure 1: Optically pumped magnetometer (OPM)- and superconducting quantum interference device (SQUID)-based magnetoencephalography (MEG) simulation in a nonparticipant 8-year-old boy. **(A)** Photograph of the magnetically shielded room dedicated to OPM recordings. **(B)** Photograph of the boy wearing the flexible electroencephalography (EEG)-like cap used for OPM-based MEG recordings. **(C)** Photograph of the three-dimensional-printed plastic mount sewn on the EEG cap, housing one OPM oriented radially. **(D)** Photograph of the three-dimensional-printed plastic mount sewn on the EEG cap without an OPM. **(E)** Photograph of the whole-scalp neuromagnetometer and magnetically shielded room used for the SQUID-based MEG recordings.

Data Preprocessing

MEG data were denoised using distinct spatial filters, which included principal components analysis for the OPMs (the first three components associated with slow, large-amplitude drifts and movement artifacts were removed) and signal space separation with movement correction (Maxfilter, MEGIN) for SQUIDs (10). Signals were band-pass filtered at 3–40 Hz. For comparability with OPM-MEG, SQUID-MEG was restricted to 102 magnetometers.

The MRI scan was manually coregistered (using anatomic fiducials for initial estimation and head surface points to manually refine the coregistration) to OPM-MEG and SQUID-MEG separately, using their respective digitalization (MRILab, MEGIN). Forward models were computed for both modalities using the one-layer boundary element method (MNE; https://mne.tools/0.17/manual/source_localization/inverse.html) (11) based on MRI tissue segmentation (FreeSurfer [12]). For OPM-MEG, sensor locations and orientations were estimated from the digitalization.

Data Analysis

IEDs were visually identified in magnetometer (32 for OPM-MEG and 102 for SQUID-MEG) signals by a resident in neurology (O.F.) and confirmed by a clinical magnetoencephalographer (X.D.T., with 15 years of experience) after consensus agreement. A spike-wave index was computed for each data set (ie, OPM-MEG and SQUID-MEG) and each participant as the ratio between the number of seconds with IEDs and the number of seconds of the total recording (13). Data were epoched from –300 to 300 msec after each spike event, baseline corrected (from –100 to –50 msec), and, finally, averaged (all or approximately 200 IEDs, depending on frequency). The neural source at the peak of the averaged spikes, and of some (all or approximately 200 IEDs, depending on frequency) individual spikes, was localized using custom-made dynamic statistical parametric mapping (14) (noise covariance estimated from baseline data, regularization from the global SNR [15]) implemented in MATLAB version 2016a (The

MathWorks). For SQUID-MEG, source reconstruction was done based on 102 magnetometers and then on 306 channels. It was also complemented with equivalent current dipole modeling of some (all or 50 IEDs, depending on frequency) individual spikes (Source Modeling, MEGIN) based on all sensors.

Statistical Analysis

For each participant, the peak amplitude and SNR of IEDs were estimated at each spike for the magnetometer showing the maximum averaged spike amplitude and compared across modalities using two-sided unpaired *t* tests; $P < .05$ was considered indicative of a statistically significant difference. This allowed comparison of two unequal sets (OPM-MEG vs SQUID-MEG) of IEDs for each participant. Finally, the distance between the reconstructed neural sources of IEDs and the closest magnetometer was estimated in order to assess how much closer OPM sensors were to the brain compared with SQUID.

Results

Participant Characteristics

Five children (median age, 9.4 years [range, 5–11 years]; four girls) were included in the study (Table 1). Three participants had self-limited genetic focal epilepsy, while the other two had RFE of unknown cause. Of those two, one (participant 2) had focal hypometabolism on fluorine 18 fluorodeoxyglucose PET scans concordant with the PLEZ but with normal structural findings at 3-T MRI of the brain, and the other (participant 5) was not seizure-free after resection of a right temporal dysembryoplastic neuroepithelial tumor with a distant PLEZ. Three participants had epileptic encephalopathy (16).

MEG Results

OPM-MEG was operator- and child-friendly, with recordings that were well tolerated by all children. The OPM localization procedure took approximately 10 minutes for each child. No

Table 1: Clinical Characteristics of Participants

Participant No.	Age (y)/Sex	Age at Seizure Onset (y)	Type of Epilepsy
1	11/M	7	SL-ECTS
2	11/F	0	Nonlesional RFE
3	5/F	3	SL-ECTS
4	9/F	8	SL-ECTS
5	11/F	7	Lesional RFE

Note.—RFE = refractory focal epilepsy, SL-ECTS = self-limited epilepsy with centrotemporal spikes.

misalignment of the three small marks drawn on the children's foreheads and the EEG cap was noticed. Unifocal and monomorphic IEDs were found in all children (spike-wave index: 2%–89%) (Figs 2, E1 [online]). At the sensor level, IEDs had comparable magnetic field topographies for both types of magnetometers (Figs 2, E1 [online]) and were consistent with that at previous clinical EEG. The IED amplitude was systematically higher (2.3 [7.2 of 3.1] to 4.6 [3.2 of 0.7] times higher, $P < .001$) with OPM-MEG than SQUID-MEG (Figs 2, E1 [online]). Additionally, the SNR was higher with OPM-MEG (27% [16.7 of 13.2] to 60% [12.8 of 8.0] higher, P value range: .001–.009) in all participants but one (participant 4).

At the source level, the distance of the neural source of the averaged IED peaks ranged from 4.2 mm to 15.6 mm between OPM-MEG and SQUID-MEG (magnetometers only) reconstructed sources (Table 2; Figs 2, E1, and E2 [online], which shows a qualitative comparison of reconstructed sources based on isolated spikes and equivalent current dipole modeling). For SQUID-MEG, the mean distance of the neural source of averaged IED peaks reconstructed with magnetometers only and all 306 sensors ranged from 1 mm to 6.7 mm (mean, 3 mm). The mean distance between the reconstructed neural source and the closest magnetometer was 29.4 mm for OPM-MEG and 57.6 mm for SQUID-MEG.

Discussion

Our study aimed to compare the ability of multichannel optically pumped magnetometer (OPM)–based magnetoencephalography (MEG) to detect and localize interictal epileptiform discharges (IEDs) in five school-aged children who have focal epilepsy with that of superconducting quantum interference device (SQUID)–based MEG (SQUID-MEG). OPM-MEG provided higher IED amplitude in all participants and a higher IED signal-to-noise ratio in all but one participant and located similar or close neural sources of IEDs. This was achieved despite a smaller number of sensors (32 OPM vs 102 SQUID magnetometers) and consequent limited scalp coverage.

To fit routine clinical practice for epilepsy, we adapted the EEG cap (7,8) for on-scalp OPM-MEG recordings. The lightweight and flexible cap design contributed to the excellent tolerance of OPM-MEG by children with epilepsy. The OPM mount design also facilitated the OPM localization procedure, which was reasonably quick (approximately 10 minutes) and well tolerated.

IEDs were detected in all participants with comparable spike-wave indexes but higher IED peak amplitudes (2.3–4.6 higher) when comparing OPM-MEG with SQUID-MEG. This reflects the reduced (approximately 3 cm on average) brain-to-sensor distance afforded by using OPMs (4). Nevertheless, OPM signals were generally noisier than SQUID signals, although the intrinsic sensor noise was similar (17) because children were allowed to move freely and the consequent movements created signal artifacts commensurate to the (<15 nT) background magnetic environment. In contrast, SQUIDs were fixed and subjected to efficient software denoising (10). Despite these disadvantages, the IED peak SNR remained significantly higher with OPM-MEG in four children and was similar to that of SQUID-MEG in the fifth child (participant 4), whose head movements created pronounced motion artifacts. This suggests that our OPM-MEG setup is adequate for pediatric recordings of IEDs. Movement-related artifacts in OPM signals could be reduced with extra hardware solutions, such as field nulling coils (4) in the magnetically shielded room (to reduce its background field <1 nT and consequently reduce movement artifacts) and OPM denoising algorithms (18,19).

Differences in the location of IED-reconstructed neural sources based on OPM-MEG and SQUID-MEG signals were in the range of SQUID-MEG spatial resolution (ie, approximately 5 mm; three participants) or higher (two participants). The latter could be related to different IED neural generators (nonsimultaneous recordings), differences in the number and spatial coverage of sensors, inaccuracies in the digitization procedure leading to inaccuracies in source reconstruction, or the higher SNR of OPM signals. Nevertheless, OPM-MEG based on 32 sensors placed around the PLEZ can help identify similar IED neural generators compared with SQUID-MEG.

There are limitations to our study. First, the number of included children was small. Second, it was difficult to compare the sensitivity of IED detection between modalities because of nonsimultaneous recordings. Third, we did not compare OPM-MEG data with a reference standard (eg, intracranial recording, resection cavity), pediatric SQUID-MEG, or scalp EEG source reconstruction. Finally, our study was limited by the number and spatial coverage of OPMs.

In conclusion, with on-scalp optically pumped magnetometer (OPM)–based magnetoencephalography (MEG), interictal epileptiform discharges were detected in school-aged children with epilepsy with a higher amplitude, higher signal-to-noise

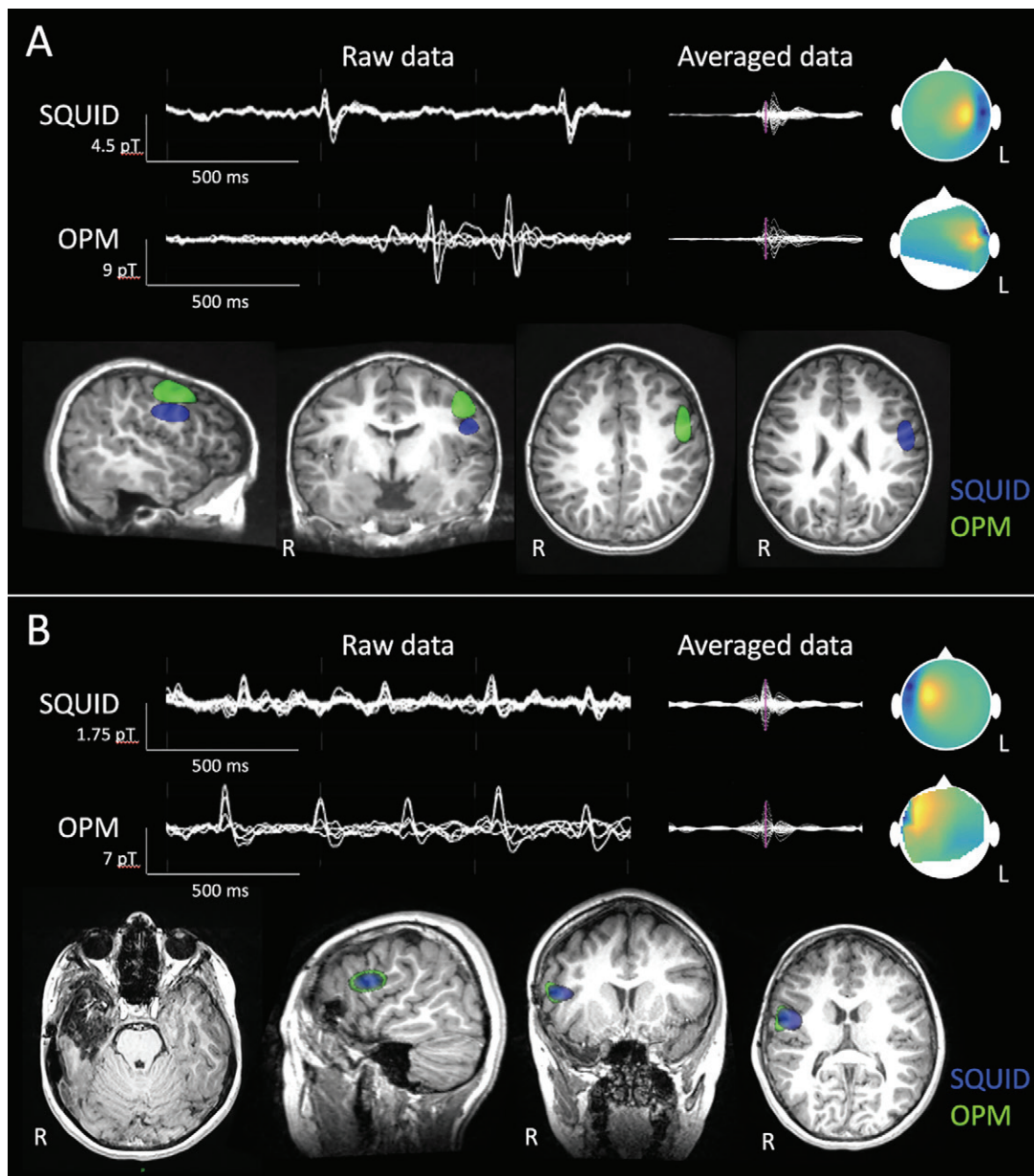


Figure 2: Optically pumped magnetometer (OPM)- and superconducting quantum interference device (SQUID)-based magnetoencephalography (MEG) data. **(A)** Images in a 5-year-old girl (participant 3) with self-limited epilepsy with centrotemporal spikes. Samples (top, left) show filtered (band-pass: 3–40 Hz) background brain activity and interictal epileptiform discharges (IEDs) recorded with SQUID-based MEG (hereafter, SQUID-MEG) and OPM-based MEG (hereafter, OPM-MEG); signals from a selected group of magnetometers were superimposed for both. Samples (top, right) show averaged IED signals and the magnetic field topography (sensor array viewed from top, arbitrary scale) at the spike peak (purple vertical line). Neural source reconstructions obtained at the averaged IED peak are displayed on parasagittal (bottom, left; left hemisphere), coronal (bottom, middle), and two axial (bottom, right) three-dimensional T1-weighted MRI scans of the brain. The distance between the locations of maximum source activity for OPM-MEG and SQUID-MEG was 15.6 mm. **(B)** Images in an 11-year-old girl (participant 5) with refractory focal epilepsy. Samples (top, left) show filtered (band-pass: 3–40 Hz) background brain activity and IEDs recorded with SQUID-MEG and OPM-MEG; signals from a selected group of magnetometers were superimposed for both. Samples (top, right) show averaged IED signals and the magnetic field topography (sensor array viewed from top, arbitrary scale) at the spike peak (purple vertical line). Axial T1-weighted MRI scan of the brain (bottom, left) shows the resection cavity after resection of a right temporal dysembryoplastic neuroepithelial tumor. Source reconstructions with OPM-MEG and SQUID-MEG are displayed on parasagittal (bottom, middle left; right hemisphere), coronal (bottom, middle right), and axial (bottom, right) three-dimensional T1-weighted MRI scans of the brain. The distance between the locations of maximum source activity for OPM-MEG and SQUID-MEG was 5.4 mm. pT = picotesla.

Table 2: Results of MEG Investigations

Participant No.	IED	Spike-Wave Index (%)		Distance between Sources and Sensor (mm)		Distance between Sources Reconstructed with OPM-MEG and SQUID-MEG (mm)	IED Amplitude (pT)*		IED SNR*		P Value†
		OPM	SQUID	OPM	SQUID		SQUID-MEG	OPM-MEG	SQUID-MEG	OPM-MEG	
1	L, CT	6	5	31.9	67.1	4.4	3.0 ± 0.08	9.9 ± 0.19	13.2 ± 0.82	16.7 ± 0.86	.004
2	L, F	3	2	33.2	64.2	8.3	0.7 ± 0.06	3.2 ± 0.21	8.0 ± 0.96	12.8 ± 1.60	.009
3	L, CT	55	47	24.5	48.7	15.6	3.1 ± 0.09	7.2 ± 0.17	9.3 ± 0.40	11.8 ± 0.51	.001
4	L, CT	5	5	30.9	60.9	4.2	1.5 ± 0.06	3.8 ± 0.21	11.3 ± 0.89	11.4 ± 1.15	.93
5	R, CT	89	85	26.1	56.8	5.4	1.8 ± 0.07	7.7 ± 0.12	11.1 ± 1.22	15.0 ± 0.74	.008

Note.—The duration of MEG recording was 30 minutes in all participants but participant 3, whose duration was 18 minutes. CT = centrotemporal, F = frontal, IED = interictal epileptiform discharge, L = left, MEG = magnetoencephalography, OPM = optically pumped magnetometer, OPM-MEG = OPM-based MEG, pT = picotesla, R = right, SNR = signal-to-noise ratio, SQUID = superconducting quantum interference device, SQUID-MEG = SQUID-based MEG.

* Data are means ± SDs.

† OPM-MEG versus SQUID-MEG IED SNR.

ratio, and similar localization value compared with conventional cryogenic MEG. Future studies based on larger numbers of patients with epilepsy and greater numbers of OPMs, to allow whole-head coverage (including the development of triaxial OPM sensors [19]), are needed to position OPM-MEG as a reference method for the diagnostic evaluation of focal epilepsy and to replace cryogenic MEG, as well as scalp electroencephalography in certain circumstances.

Author contributions: Guarantors of integrity of entire study, **O.F., S.G., X.D.T.**; study concepts/study design or data acquisition or data analysis/interpretation, all authors; manuscript drafting or manuscript revision for important intellectual content, all authors; approval of final version of submitted manuscript, all authors; agrees to ensure any questions related to the work are appropriately resolved, all authors; literature research, **O.F., A.A., M.B., S.G., V.W., X.D.T.**; clinical studies, **O.F., A.A., C.S., F.C., S.G., X.D.T.**; experimental studies, **O.F., P.C., N.H., M.B., V.W., X.D.T.**; statistical analysis, **O.F., V.W., X.D.T.**; and manuscript editing, **O.F., P.C., A.A., N.H., M.B., S.G., V.W., X.D.T.**

Disclosures of conflicts of interest: **O.F.** No relevant relationships. **P.C.** No relevant relationships. **A.A.** No relevant relationships. **C.S.** No relevant relationships. **F.C.** No relevant relationships. **N.H.** Cofounder and scientific advisor for Cerca Magnetics Limited. **M.B.** Nonexecutive chairman for Cerca Magnetics Limited. **S.G.** No relevant relationships. **V.W.** No relevant relationships. **X.D.T.** Clinical researcher at the FRS-FNRS.

References

1. Tamilia E, AlHilani M, Tanaka N, et al. Assessing the localization accuracy and clinical utility of electric and magnetic source imaging in children with epilepsy. *Clin Neurophysiol* 2019;130(4):491–504.
2. Burgess RC. MEG for Greater Sensitivity and More Precise Localization in Epilepsy. *Neuroimaging Clin N Am* 2020;30(2):145–158.
3. Rampf S, Stefan H, Wu X, et al. Magnetoencephalography for epileptic focus localization in a series of 1000 cases. *Brain* 2019;142(10):3059–3071.
4. Boto E, Holmes N, Leggett J, et al. Moving magnetoencephalography towards real-world applications with a wearable system. *Nature* 2018;555(7698):657–661.

5. Gaetz W, Gordon R, Papadelis C, et al. Magnetoencephalography for Clinical Pediatrics: Recent Advances in Hardware, Methods, and Clinical Applications. *J Pediatr Epilepsy* 2015;04(04):139–155.
6. Vivekananda U, Mellor S, Tierney TM, et al. Optically pumped magnetoencephalography in epilepsy. *Ann Clin Transl Neurol* 2020;7(3):397–401.
7. Hill RM, Boto E, Rea M, et al. Multi-channel whole-head OPM-MEG: Helmet design and a comparison with a conventional system. *Neuroimage* 2020;219:116995.
8. Boto E, Hill RM, Rea M, et al. Measuring functional connectivity with wearable MEG. *Neuroimage* 2021;230:117815.
9. Carrette E, Op de Beeck M, Bourguignon M, et al. Recording temporal lobe epileptic activity with MEG in a light-weight magnetic shield. *Seizure* 2011;20(5):414–418.
10. Taulu S, Simola J. Spatiotemporal signal space separation method for rejecting nearby interference in MEG measurements. *Phys Med Biol* 2006;51(7):1759–1768.
11. Gramfort A, Luessi M, Larson E, et al. MEG and EEG data analysis with MNE-Python. *Front Neurosci* 2013;7:267.
12. Fischl B. *FreeSurfer*. *Neuroimage* 2012;62(2):774–781.
13. Aeby A, Santalucia R, Van Hecke A, et al. A qualitative awake EEG score for the diagnosis of continuous spike and waves during sleep (CSWS) syndrome in self-limited focal epilepsy (SFE): A case-control study. *Seizure* 2021;84:34–39.
14. Dale AM, Sereno MI. Improved Localization of Cortical Activity by Combining EEG and MEG with MRI Cortical Surface Reconstruction: A Linear Approach. *J Cogn Neurosci* 1993;5(2):162–176.
15. Wens V, Marty B, Mary A, et al. A geometric correction scheme for spatial leakage effects in MEG/EEG seed-based functional connectivity mapping. *Hum Brain Mapp* 2015;36(11):4604–4621.
16. Scheffer IE, Berkovic S, Capovilla G, et al. ILAE classification of the epilepsies: Position paper of the ILAE Commission for Classification and Terminology. *Epilepsia* 2017;58(4):512–521.
17. Shah VK, Wakai RT. A compact, high performance atomic magnetometer for biomedical applications. *Phys Med Biol* 2013;58(22):8153–8161.
18. Rea M, Holmes N, Hill RM, et al. Precision magnetic field modeling and control for wearable magnetoencephalography. *Neuroimage* 2021;241:118401.
19. Mellor S, Tierney TM, O’Neill GC, et al. Magnetic Field Mapping and Correction for Moving OP-MEG. *IEEE Trans Biomed Eng* 2022;69(2):528–536.